Available online at www.sciencedirect.com
ScienceDirect
Procedia Computer Science 00 (2010) 1–10
Procedia Computer Science

Adaptive modeling of methane hydrates

Małgorzata Peszyńska[a,1,*], Marta Torres[b,2], Anne Trèhu[b,1]

[a] *Department of Mathematics, Oregon State University, Corvallis, OR 97331*
[b] *College of Oceanic and Atmospheric Sciences, Oregon State University, Corvallis, OR 97331*

Abstract

We consider a computational model for the evolution of methane hydrates in subsurface. Methane hydrates, an ice-like compound abundant in subsea sediments and unstable in standard conditions, are an environmental hazard and simultaneously an energy source. Our multiphysics model includes multiphase multicomponent mass conservation equations and several variants of energy balance equation with or without latent heat. We present the technique of model adaptivity which helps to assess and control the two sources of the computational error: the discretization error and the modeling error. The nature and magnitude of the modeling error is strongly dependent on the application and smoothness of solutions.

Keywords: adaptive modeling, a posteriori estimates, methane hydrate modeling, phase transitions, free boundary
2000 MSC: 65M06, 80A22,, 35Q80, 35Q35, 65N15, 65Z05, 76S99, 76T99, 76R99

1. Introduction

In this paper we consider a multiphysics computational model for methane hydrates. Methane hydrates, ice-like structures present in subsea sediments, are stable only at low temperatures and high pressures, and are an environmental hazard and an energy source [1, 2, 3]. We are interested in the assessment and control of the computational error for various variants of the model.

When modeling complex phenomena one has to assess and control two sources of computational modeling error: the discretization error and the modeling error. Consider an exact model of a complex phenomenon $\mathbf{M}(\mathbf{u}) = 0,\ \mathbf{u} \in \Upsilon$, where $\mathbf{u}$ denotes a set of primary unknowns and Υ

*Corresponding author
Email addresses: mpesz@math.oregonstate.edu (Małgorzata Peszyńska), mtorres@coas.oregonstate.edu (Marta Torres), trehu@coas.oregonstate.edu (Anne Trèhu)
URL: http://www.math.oregonstate.edu/~mpesz (Małgorzata Peszyńska)
[1] partially supported by National Science Foundation grant 0511190 and Department of Energy grant 98089
[2] partially supported by Department of Energy, NETL Grant V0292A (RDSX 11410)

the state space. In practice one solves for $\mathbf{u}_h \in \Upsilon_h$ its computational counterpart

$$\mathbf{M}_h(\mathbf{u}_h) = 0, \quad \mathbf{u}_h \in \Upsilon_h, \tag{1}$$

where $\Upsilon_h \subsetneq \Upsilon$ is of finite dimension, and h is the grid parameter. The computational error $\mathbf{u} - \mathbf{u}_h$ arises from approximation error of Υ by Υ_h as well as from the modeling approximation $\mathbf{M} \to \mathbf{M}_h$ due to, e.g., numerical integration, linearization, or decoupling.

Now consider a modified computational model $\tilde{\mathbf{M}}_h(\tilde{\mathbf{u}}_h) = 0$ which is a discretization of some modified model $\tilde{\mathbf{M}}$ close to $\mathbf{M}$, or a modification of $\mathbf{M}_h$. The idea is that the solutions $\tilde{\mathbf{u}}_h$ are easier to obtain than those of (1) and that the additional modeling error that arises is of similar order of magnitude as the discretization error for (1). To asses and control the error $\mathbf{u} - \tilde{\mathbf{u}}_h$ we can use the splittings

$$\mathbf{u} - \tilde{\mathbf{u}}_h = \underbrace{\mathbf{u} - \tilde{\mathbf{u}}}_{\textit{modeling error}} + \underbrace{\tilde{\mathbf{u}} - \tilde{\mathbf{u}}_h}_{\textit{discretization error in } \tilde{\mathbf{M}}} = \underbrace{\mathbf{u}_h - \tilde{\mathbf{u}}_h}_{\textit{discrete modeling error}} + \underbrace{\mathbf{u} - \mathbf{u}_h}_{\textit{discretization error in } \mathbf{M}} .$$

The discretization error(s) $\mathbf{u} - \mathbf{u}_h$ or $\tilde{\mathbf{u}} - \tilde{\mathbf{u}}_h$ can be estimated and controlled via a-posteriori error estimators and grid adaptivity techniques which are most successful for linear scalar model problems but are nontrivial to formulate for highly nonlinear coupled problems, see [4, 5, 6, 7] for representative references for model problems.

However, it is not obvious how to handle the modeling error $\mathbf{u} - \tilde{\mathbf{u}}$ or $\mathbf{u}_h - \tilde{\mathbf{u}}_h$; its nature and magnitude is strongly application dependent and this error may be expensive to estimate except for simple model scalar problems. As an *indicator* of the modeling error we propose to use $\mathbf{u}_H - \tilde{\mathbf{u}}_H$ which is relatively inexpensive to obtain if $H >> h$. Theoretical foundation can be found in [8]; in this paper we present an illustration how this works for a complex system.

Specifically, let (1) represent a coupled transient system of nonlinear partial differential equations (PDEs) describing the evolution of methane hydrates in subsurface. Some of the components $(\mathbf{u})_c$ of the unknowns $\mathbf{u}$ may exhibit sharp fronts while some others may be smooth enough to be measured in energy norm. In addition, we cannot expect differentiability of solutions of PDEs with respect to just any parameter of that PDE. Therefore, the influence of one component upon the others, and/or the impact of model modifications, when assessed via sensitivity analysis, is based on only a very weak theoretical foundation. In this paper we discuss a few qualitative ideas for assessing the modeling error.

The plan of the paper is as follows. We first present the model of methane hydrates in which diffusion and phase transitions dominate. We solve mass conservation equations and an energy balance in four variants which represent various model modifications $\tilde{\mathbf{M}}$ of a basic model $\mathbf{M}$. Then we propose how to assess the global computational modeling error.

Last, we comment on the state of the art of methane hydrate modeling. The simulators such as STOMP-MH [9] and TOUGH+Hydrate [10] have computational models based on finite volumes and state-of-the-art thermodynamics and solver capabilities. On the other hand, recent research codes [11, 12] are concerned with important scenarios of hydrate evolution. However, little is known about the error analysis and control, or about the impact of model modifications in these implementations. This paper is a step in this direction, but the ideas have been applied only to a simplified model. The significant challenge will be to incorporate the model and grid adaptivity ideas proposed here in a comprehensive fully implicit implementation.

2. Mathematical model for hydrate evolution, static temperature

Here we briefly present a model for hydrate evolution in subsurface. We follow closely the standard notation for multiphase, multicomponent flow and transport as in [13, 14, 15]. A comprehensive model for hydrates such as [9, 10, 11, 12] may include all the first-order and many second- or third-order effects relevant at various time scales of interest. In this paper we consider only first order effects relevant at large time scales [1] such as diffusion and phase transitions and account for temperature evolution, but ignore sedimentation rate. We note that the model in [11] does not include latent heat while we were not able to identify all the necessary definitions of energy-related terms in [12].

We consider methane and other fluids in a porous subsea sediment reservoir $\Omega \subset \mathbb{R}^d$, $1 \leq d \leq 3$, an open bounded domain. The reservoir is under the earth surface; its depth is denoted by $D(\mathbf{x}), \mathbf{x} \in \Omega$, and its porosity and permeability by $\phi, \mathbf{K}$, respectively. In this paper we assume $\phi = const, \mathbf{K} = const$.

2.1. Phases and components

In addition to methane M, the main components of the fluids in the porespace are water W and salt S. These can be present in one or more phases. In general, in [11, 12] one considers two mobile fluid phases l, g (brine, gas) and an immobile hydrate phase h (hydrate). Usually the pore space is mainly saturated with water phase with only a small amount of methane gas present. The three phases l, g, h occupy together the pore space and their respective volume fractions are denoted by saturations $S_p, p = l, g, h$, with $S_p \geq 0$, and $\sum_p S_p = 1$.

Usually one considers phase pressures of mobile phases P_l, P_g, and the capillary pressure relationship $P_g - P_l = P_c(S_l)$ given by Brooks-Corey relationships or van-Genuchten correlations [13]. The advective velocities are given via a multiphase extension of Darcy's law $\mathbf{v}_p = -\mathbf{K}\frac{k_{rp}}{\mu_p}(\nabla P_p - \rho_p G \nabla D(\mathbf{x})), p = l, g$, where k_{rp}, μ_p denote relative permeability, viscosity, and density of phase p and G the gravity constant. In this paper we assume $\rho_p = const$.

In this paper we assume that the water phase is distributed hydrostatically, i.e., the gradient of the potential in Darcy's law is zero and therefore $\mathbf{v}_l = 0$. In addition, we assume that the gas phase saturations are below their residual amount i.e. gas phase is immobile due to $k_{rg} \equiv 0$ and $\mathbf{v}_g = 0$. In other words both phases are effectively immobile. Any mass transfer occurs by diffusion in liquid phase and by phase transition to gas and hydrate phases. In what follows we also set $P = P_l$ and ignore capillary pressure i.e. $P_g = P$.

To account for component diffusion and component distribution between phases and for phase transitions, we discuss mass of each component. Mass fraction of component C in phase p is denoted by X_{pC}, and we have $X_{pC} \geq 0$. We have for each phase p, $\sum_C X_{pC} = 1$, and specifically in this paper

$$X_{gM} = 1, \quad \text{(gas phase contains methane only)} \tag{2}$$

$$X_{hM} + X_{hW} = 1, \quad \text{(both known for a fixed hydrate nuumber)} \tag{3}$$

$$X_{lM} + X_{lW} + X_{lS} = 1, \quad \text{(unknown variables).} \tag{4}$$

2.2. Thermodynamics

The distribution of components between phases is governed by thermodynamics. In particular, one needs the following quantities to determine phase behavior: i) the equilibrium (melting/dissociation) pressure for given T and salinity $P^{EQ} = P^{EQ}(T, X_{lS})$, and ii) maximum solubility $X_{lS}^{max}(P, T, X_{lS})$ of methane M in liquid phase $p = l$. Such data is available in the literature via

various functional models related to an equation of state (EOS) approach, or via lookup tables [2, 12, 16, 17].

2.3. Mass conservation equations

The general phase-summed mass conservation equation is

$$storage_C + advection_C + diffusion_C = source_C,$$

where the individual terms vary with $C = M, W, S$. Dropping the advection terms we have

$$\overbrace{\frac{\partial}{\partial t}(\phi S_g \rho_g + \phi S_l \rho_l X_{lM} + \phi S_h \rho_h X_{hM})}^{storage_M} - \overbrace{\nabla \cdot (D_m \phi S_l \rho_l \nabla X_{lM})}^{diffusion_M} = 0 \quad (5)$$

$$\overbrace{\frac{\partial}{\partial t}(\phi S_l \rho_l X_{lS})}^{storage_S} - \overbrace{\nabla \cdot (D_s \phi S_l \rho_l \nabla X_{lS})}^{diffusion_S} = 0. \quad (6)$$

These equations describe diffusive mass transfer of methane M and of salt S in liquid phase $p = l$; the definition of diffusive fluxes follows from Fick's law.

Formally we can also write for the water component $\frac{\partial}{\partial t}(\phi S_l \rho_l (1 - X_{lS} - X_{lW})) = 0$. Adding this equation to (6), (5), in case of nontrivial advective fluxes would yield an equation for the pressure. However, since the pressure is assumed hydrostatic and advective fluxes vanish, X_{lS} and X_{lM} can be found from (6)–(5), and the water equation is redundant.

If P, T are known, the system (5)–(6), when complemented with initial and boundary conditions, can be solved numerically. To fix the pressure, we assume hydrostatic pressure model $P_0(\mathbf{x})$ linear with depth via hydrostatic gradient: $P_{top} = 8MPa$, and lithostatic/hydrostatic gradient is 10.4MPa/km which gives bottom pressure at depth of $400m$ of about 10MPa. Similarly, we assume a fixed thermal gradient and an associated static linear temperature profile $T_0(\mathbf{x})$. with $T_{top} = 4^oC$ and geothermal gradient $55^oC/km$ which gives the bottom temp about 11^oC, see example in Figure 1.

After discretization, the resulting algebraic system is solved for two primary variables which fully describe the thermodynamic conditions in the model; see Gibbs rule [18, 13, 19]. The choice of primary variables $\mathbf{u}$ may be dictated by convenience but it must be possible to compute all other variables from $\mathbf{u}$. The choice which variables are primary is tricky when phases appear/disappear in certain parts of Ω; this is a long-standing issue in reservoir simulation.

In [14, 20, 15] variable switching is proposed. Here we follow another approach used in petroleum industry [21, 22, 23]: we define concentrations N_C which are the storage terms under $\frac{\partial}{\partial t}$ in (5) and use these as primary unknowns. Concentrations are smoother than phase saturations but their use may require a local nonlinear solver called *flash*, see [23, 13].

An example of hydrate evolution similar to scenarios in [11] is shown in Figure 1.

2.4. Solving the coupled nonlinear system

Now consider the discretization of the equations (5)-(6). Both spatial and temporal grids are adaptive but are assumed uniform in the presentation below. To discretize in space, we apply the cell-centered finite difference method; this method is conservative, equivalent to mixed finite elements on rectangular grids [24], and is amenable to adaptivity [25]. Also, it can be easily extended to a more general model with advection. For time discretization, one can apply either

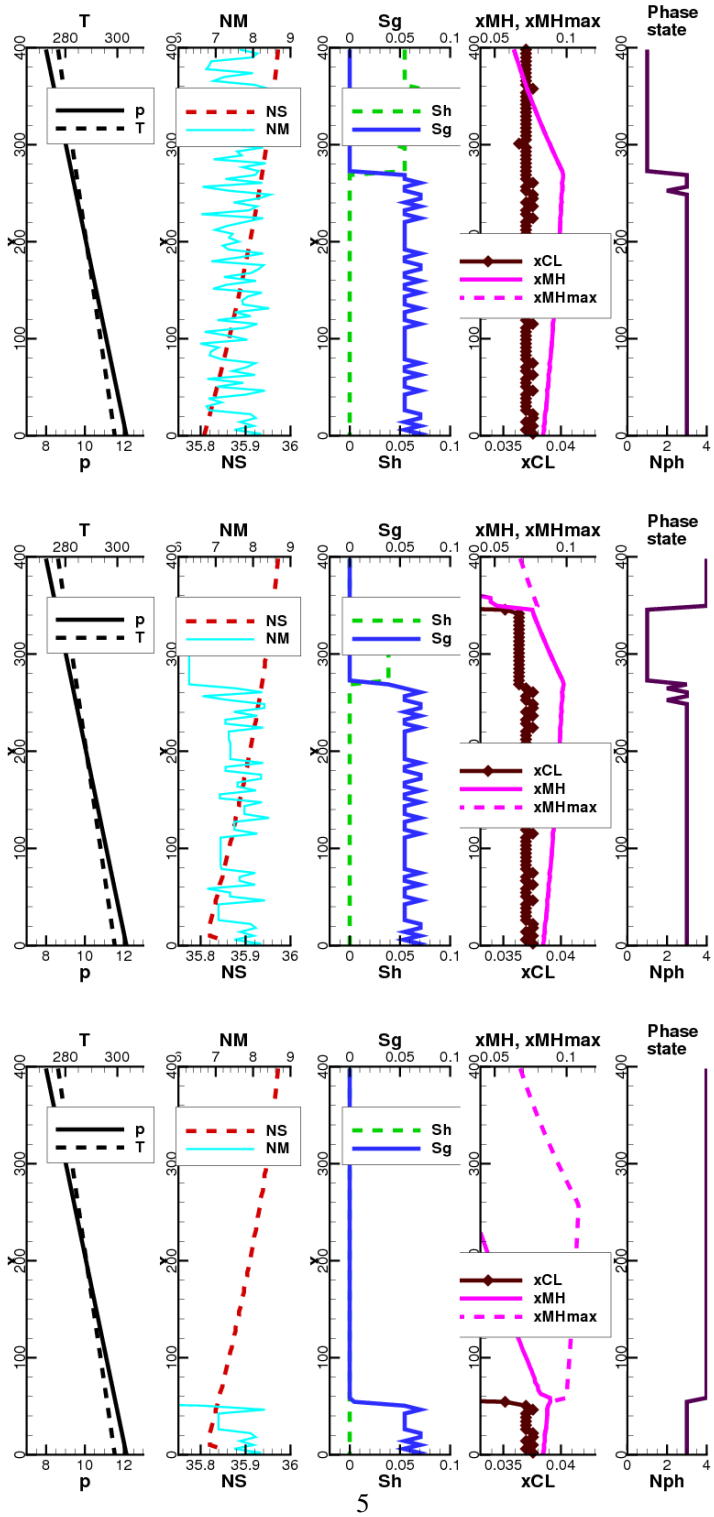

Figure 1: Evolution of methane hydrates. Shown are profiles of temperature, pressure, gas and hydrate saturations, solubilities, and phase state, at time step 1, 10, 100 (nondimensional). Phase state is 1 (L+H), 2 (L+H+G), 3 (L+G), 4 (L). The methane concentration N_M is decreasing because we let it escape it to the ocean at $x = 400$. This causes the dissociation of hydrate and the decrease in salinity; the hydrate/gas interface moves down.

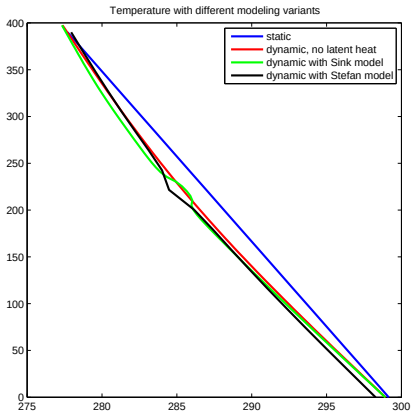

Figure 2: Temperature profiles for different variants of energy equation. Static model uses (9). Dynamic, no latent heat model, uses (11) with $L_H = 0$. Dynamic, sink-type model, uses (11). Dynamic, Stefan-type model, uses $\tilde{L}_H$. Not shown is grid convergence of tempreatures in energy norm which is global for models without latent heat, and local away from phase boundary for the models with latent heat.

a fully implicit formulation or a sequential formulation. Either way, the most difficult part of the model is accounting for all the correct thermodynamics and phase transition behavior.

Fully implicit formulation has the advantage of being unconditionally stable while it requires a substantial computational effort and may be overly diffusive; it is advocated for production-quality simulations of a comprehensive model with second and third order effects [9, 10]. In this paper we report on the results of a sequential formulation which shows the first order effects quite well and can be naturally imbedded in our model adaptivity procedure. We use a very small time step to practically eliminate the time discretization error, and to ensure stability.

For (5)-(6) combined with the static profile of temperature, with the notation related to the spatial discretization supressed, we solve the following system at time step t_{n+1}

$$F_M^n(N_M^{n+1}) = 0, \tag{7}$$
$$F_S^n(N_S^{n+1}) = 0, \tag{8}$$
$$T^{n+1} = T_0(\mathbf{x}). \tag{9}$$

Here F_C^n denotes a collection of accumulation and diffusion terms whose coefficients are evaluated at the time step t_n for the component $C = M, S$. The linear solver is applied to resolve the resulting set of systems of linear equations for N_M^{n+1}, N_S^{n+1} which approximate the true values at the time step t_{n+1}.

3. A model for methane hydrates with dynamic energy balance

Now we replace (9) by one of several variants of a dynamic energy balance equation; its importance is discussed in [26, 27]. These various models replace (9) by the energy equation of the form $F_T^{n+1/2}(T_h^{n+1}) = 0$, in several variants.

A general energy equation for multiphase multicomponent system has a structure similar to (5) with heat conduction terms en lieu of diffusive terms and convective fluxes en lieu of

advective fluxes, now associated with the overall mass flux term $\mathbf{F}$

$$\frac{\partial}{\partial t}(C(T)) + \nabla \cdot (H\rho\mathbf{F}) - \nabla \cdot (\lambda(T)\nabla T) = 0, \tag{10}$$

in which H is the enthalpy [13, 18, 28]. We need now to make explicit the heat accumulation/capacity $C(T)$ and the heat conductivity $\lambda(T)$ terms, as well as identify the latent heat effects. The latter arise during the hydrate formation and dissociation in a process similar to water-ice phase transition.

In the classical Stefan model [28] for water-ice phase transitions occuring at a temperature T^{eq}, we have $C(T) = T \begin{cases} C_1, & T < T^{eq}, \\ C_2, & T \geq T^{eq}, \end{cases} + L\mathcal{H}(T - T^{eq})$, and $\lambda(T) = \begin{cases} \lambda_1, & T < T^{EQ}, \\ \lambda_2, & T \geq T^{EQ} \end{cases}$. Here $\mathcal{H}(\cdot)$ denotes the Heaviside graph and L denotes the latent heat of phase transition which occurs at T^{EQ}. The model only has weak solutions as the graph $\mathcal{H}(T)$ is not differentiable in a classical sense; its distributional derivative is a Dirac source concentrated along the free boundary and the analysis is highly nontrivial; see [29, 28] for a few representative references. Appropriately, numerical solution is delicate; the use of adaptive methods and various regularizations in particular with phase-field models or level-set methods have been considered e.g. in [30, 31, 32].

Consider the behavior of solutions to (10) when initially the region Ω is occupied by ice under $T(\mathbf{x}, 0) = T_0 < T^{EQ}$. In a model driven by heat supplied from one of the boundaries, while the other boundary is kept at T_0, the free boundary between the regions occupied by water and ice moves in time and eventually assumes a stationary profile across which the temperature T is continuous but its gradient is not. The profile of the dynamic solutions $T(\mathbf{x}, t)$ depends on the magnitude of L. However, in the absence of mass fluxes, the stationary solution $T(\mathbf{x}, \infty) := \lim_{t\to\infty} T(\mathbf{x}, t)$ does not depend on L but only on the jump $\lambda_1 - \lambda_2$ in $\lambda(T)$. In other words, one can find $T(\mathbf{x}, \infty)$ with a model including latent heat or not; this suggests opportunities for model adaptivity if one is interested only in long-term solutions.

An appropriate extension of Stefan-type model to multiple phases and components [13, 18] includes summation over phases and phase enthalpies $H_p = C_p T$ so that $C(T) = (1-\phi)\rho_R C_R T + \phi \sum_{p=l,g,h} S_p \rho_p C_p T$, $\lambda(T) = (1-\phi)\lambda_R + \phi \sum_{p=l,g,h} S_p \lambda_p$. These definitions are refined further to identify the latent heat of hydrate dissociation L_H as the difference of enthalpies $H_h - H_l$. We skip the details and consider the following definition of rate of change of $C(T)$ [13, 18]

$$\frac{\partial}{\partial t}(C(T)) = \frac{\partial}{\partial t}(C_T T) + L_H \frac{\partial}{\partial t}(\phi S_h \rho_h), \tag{11}$$

where we have used the total heat capacity $C_T := (1-\phi)\rho_R C_R T + \phi \sum_{p=l,g,h} S_p \rho_p C_p$.

The mass conservation combined with (10) and (11) is our reference model $\mathbf{M}(\mathbf{u}) = 0$. We refer to it as the Sink-type model [33, 34], because the term $L_H \frac{\partial}{\partial t}(\phi S_h \rho_h)$ plays a role of a heat sink term when moved to the right-hand side of (10).

A simple modification of $\mathbf{M}$ is the dynamic model $\tilde{\mathbf{M}}^{dynamic}$ obtained from $\mathbf{M}$ when we set $L_H = 0$. An even simpler version $\tilde{\mathbf{M}}^{static}$ discussed in previous section replaces the energy equation in $\mathbf{M}$ by (9); its results are shown in Figure 1. Yet another variant $\tilde{\mathbf{M}}^{STEFAN}$ or a Stefan-like model accounts only for the occurence of phase transition and not accurately for its magnitude. It is derived [3] when the sink term is replaced by $\tilde{L}_H \frac{\partial}{\partial t}(\mathcal{H}(T - T^{EQ})$ where $\tilde{L}_H$ accounts for volume and mass change.

It is very interesting to compare the solutions corresponding to $\mathbf{M}, \tilde{\mathbf{M}}^{static}, \tilde{\mathbf{M}}^{dynamic}, \tilde{\mathbf{M}}^{STEFAN}$. Figures 2 and 3 present plots of results using data similar to those in Figure 1 with the following modifications: we assume a constant initial amount of methane N_M, and the initial temperature

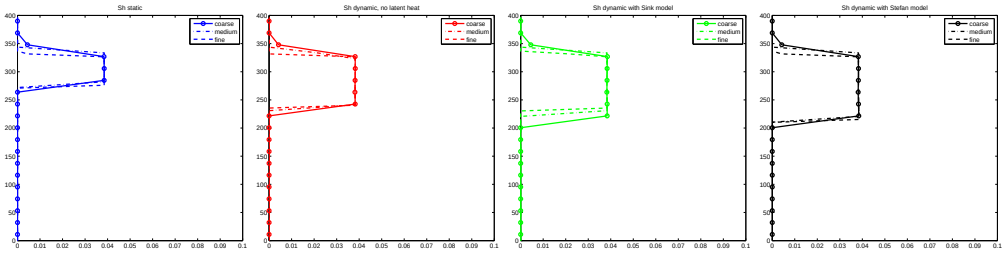

a) b) c) d)

Figure 3: Saturation profiles for different temperature models with a) static, b) dynamic, no latent heat, c) dynamic, with sink model and d) dynamic, with Stefan-like model. Visible is (weak) grid convergence of saturations.

at sea bottom lower by $3^o K$ than the final temperature. The temperature rises according to the energy equation in all models except $\tilde{\mathbf{M}}^{static}$. The values of temperature and saturations are shown at the (nondimensional) time step $t_n = 10$.

4. Adaptive modeling of Methane Hydrate

When considering adaptive modeling and grid refinement, the first concern is whether the convergence in discretization parameters can be indeed observed and in what norm it should be measured. Theory suggests that for smooth solutions one can expect at least first order convergence in L^2 or even H_1 norm. At the same time, non-smooth components may not converge in norms stronger than L^1.

In our problem, an example of smooth and non-smooth variables is provided by the temperatures and the hydrate saturations, see Figures 2, 3, respectively. The former are continuous and smooth except near the phase transition boundaries, and the latter exhibit a sharp change at the boundary where the hydrate dissociates and forms. Therefore, it is not possible to apply simple a-posteriori error estimates to both variables.

Now we focus on the modeling error and the combined computational error and provide an illustration of the ideas given in Introduction applied to our complex coupled problem. We discuss the total pointwise error $\tilde{e}^c_h = (\mathbf{u} - \tilde{\mathbf{u}}_h)_c$ and the qualitative behavior of the grid error combined with the modeling error for the selected components c of $\mathbf{u}$. The exact value $\mathbf{u}$ is estimated from a very fine grid solution (not shown), after we test the stability of solutions. We consider the error(s) $\tilde{e}^T_h$ in the temperature T variable which is a smooth component of $\mathbf{u}$, and $\tilde{e}^{S_h}_h$ in the hydrate saturation S_h, which is nonsmooth. The errors are shown for two grids: the coarse grid H and medium grid h, with interpolation used as needed. The goal is to understand the behavior of error on the medium grid h by using the inexpensive estimates of the error on the coarse grid.

In Figure 4 we show the pointwise error $\tilde{e}^c_H := ((\mathbf{u} - \mathbf{u}_H) + (\mathbf{u}_H - \tilde{\mathbf{u}}_H))_c$ for both components which includes the grid plus the modeling error on the coarse grid. We see that $\tilde{e}^c_H$ agrees well qualitatively with $\tilde{e}^c_h$ for both variables $c = T, S_h$.. However, the grid error is overpredicted significantly when measured in the energy norm, or in L^p, $p = 1$ norms, for smooth and nonsmooth components, respectively. Therefore, we need an indicator for the grid error on medium grid, and the modeling error on the coarse grid $\eta^c_{Hh} := (\mathbf{u} - \mathbf{u}_h)_c S(h, H) + (\mathbf{u}_H - \tilde{\mathbf{u}}_H)_c$. Here the scaling coefficient $S(h, H)$ reflects the anticipated order of convergence; e.g., should equal $\frac{H}{h}$ for a smooth component converging linearly. For a nonsmooth variable, we use $S(h, H) \equiv 1$.

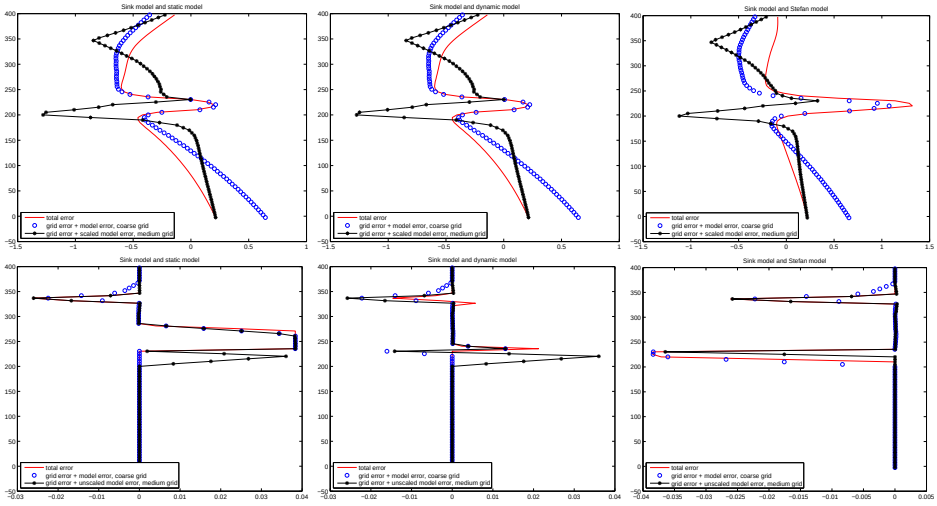

Figure 4: Total pointwise error e_h^c and its indicators e_H^c and η_{Hh}^c for $c = T$ (top) and $c = S_h$ (bottom). From left to right: comparison of the base case (Sink model) to the static, dynamic, and Stefan models.

While these illustrations are only qualitative, we see that for a very crude modeling approximation (e.g. static versus Sink model) the modeling error dominates and the total error can be assessed on a coarse grid. The more subtle modeling error between the dynamic and Stefan models needs an indicator such as η_{Hh}^c. More analysis is needed and some is underway.

5. Conclusions and future work

We have presented a grid-convergent computational model for evolution of methane hydrates in which we considered several variants of the energy balance equations. We have also illustrated and estimated the modeling error associated with each variant, and demonstrated general agreement in the order of magnitude of the errors as well as in their qualitative behavior.

More analysis is needed to understand the proper scaling of the modeling error in relation to the discretization error. For the methane hydrate model, further analysis of the numerical error as well as definition of fully comprehensive adaptivity case studies are needed; some results in this direction are underway.

Other opportunities for adaptivity of a complex model include i) the modification of thermodynamics models, ii) the use of kinetic versus equilibrium phase transition models, iii) the considerations of competition of advection and diffusion at various time scales, and many others. These are subject of our current work.

[1] M. Torres, K. Wallmann, A. Trhu, G. Bohrmann, W. Borowski, H. Tomaru, Gas hydrate growth, methane transport, and chloride enrichment at the southern summit of Hydrate Ridge, Cascadia margin off Oregon, Earth and Planetary Science Letters 226 (1-2) (2004) 225 – 241. doi:DOI: 10.1016/j.epsl.2004.07.029.

[2] E. Sloan, C. A. Koh, Clathrate Hydrates of Natural Gases, 3rd Edition, CRC Press, 2008.

[3] S. K. Kelkar, M. S. Selim, E. D. Sloan, Hydrate dissociation rates in pipelines, Fluid Phase Equilibria 150-151 (1998) 371 – 382.

[4] I. Babuska, W. C. Rheinboldt, A posteriori error analysis of finite element solutions for one-dimensional problems, SIAM J. Numer. Anal. 18 (3) (1981) 565–589.

[5] R. Verfürth, A posteriori error estimates for nonlinear problems. $Lp^*r(0,T;Lp^*\rho(\Omega))$-error estimates for finite element discretizations of parabolic equations, Math. Comp. 67 (224) (1998) 1335–1360.
[6] M. Ainsworth, J. T. Oden, A posteriori error estimation in finite element analysis, Comput. Methods Appl. Mech. Engrg. 142 (1-2) (1997) 1–88.
[7] R. Verfürth, A review of a posteriori error estimation and adaptive mesh-refinement techniques, Wiley-Teubner, Chichester, 1996.
[8] M. Peszyńska, Model adaptivity for porous media, manuscript.
[9] Stomp: Subsurface Transport Over Multiple Phases simulator website `http://stomp.pnl.gov/`, note = "[online; accessed 11-january-2010]".
[10] TOUGH Family of Codes: Availability and Licensing, `http://esd.lbl.gov/TOUGH2/avail.html`, [Online; accessed 11-January-2010].
[11] X. Liu, P. B. Flemings, Dynamic multiphase flow model of hydrate formation in marine sediments, Journal of Geophysical Research 112 (2008) B03101.
[12] S. Garg, J. Pritchett, A. Katoh, K. Baba, T. Fijii, A mathematical model for the formation and dossociation of methane hydrates in the marine environment, Journal of Geophysical Research 113 (2008) B08201.
[13] L. W. Lake, Enhanced oil recovery, Prentice Hall, 1989.
[14] R. Falta, K. Pruess, I. Javandel, P. A. Witherspoon, Numerical modeling of steam injection for the removal of nonaqueous phase liquids from the subsurgacee 1. numerical formulation, Water Res. Research 28 (2) (1992) 433–449.
[15] H. Class, R. Helmig, P. Bastian, Numerical simulation of non-isothermal ultiphase multicomponent processes in porous media 1. an efficient solution technique, Advances in Water Resources 25 (2002) 533–550.
[16] P. Tishchenko, C. Hensen, K. Wallmann, C. S. Wong, Calculation of stability and solubility of methane hydrate in seawater, Chemical Geology 219 (2005) 37–52.
[17] M. Davie, B. A. Buffett, A steady state model for marine hydrate formation: Constraints on methane supply from pore water sulfate profiles, Journal of Geophysical Research 108 (2003) B10, 2495.
[18] A. Firoozabadi, Thermodynamics of hydrocarbon reservoirs, McGraw-Hill, 1999.
[19] J. Smith, H. V. Ness, M. Abbott, Introduction to chemical engineering thermodynamics, McGraw-Hill, 1996.
[20] R. Helmig, Multiphase flow and transport processes in the Subsurface, Springer, 1997.
[21] Q. Lu, M. Peszyńska, M. F. Wheeler, A parallel multi-block black-oil model in multi-model implementation., SPE Journal 7 (3) (2002) 278–287, sPE 79535.
[22] G. Chavent, J. Jaffre, Mathematical models and finite elements for reservoir simulation, North-Holland, Amsterdam, 1986.
[23] M. Peszyńska, The total compressibility condition and resolution of local nonlinearities in an implicit black-oil model with capillary effects, Transport in Porous Media 63 (1) (2006) 201 – 222.
[24] T. F. Russell, M. F. Wheeler, Finite element and finite difference methods for continuous flows in porous media, in: R. E. Ewing (Ed.), The Mathematics of Reservoir Simulation, SIAM, Philadelphia, 1983, pp. 35–106.
[25] M. Peszyńska, Mortar adaptivity in mixed methods for flow in porous media, International Journal of Numerical Analysis and Modeling 2 (3) (2005) 241–282.
[26] K. Masataka, N. Yukihiko, G. Shusaku, A. Juichiro, Effect of the latent heat on the gas–hydrate/gas phase boundary depth due to faulting, Bulletin of Earthquake Research Institute, University of Tokyo 73.
[27] M. B. Clennell, M. Hovland, J. Booth, P. Henry, W. Winters, Formation of natural gas hydrates in marine sediments 1. conceptual model of gas hydrate growth conditioned by host sediment properties, Journal of Geophysical Research 104 (1999) 22,985–23,003.
[28] A. Visintin, Models of phase transitions, Progress in Nonlinear Differential Equations and their Applications, 28, Birkhäuser Boston Inc., Boston, MA, 1996.
[29] E. DiBenedetto, R. E. Showalter, A pseudoparabolic variational inequality and Stefan problem, Nonlinear Anal. 6 (3) (1982) 279–291.
[30] R. H. Nochetto, C. Verdi, Approximation of multidimensional Stefan-like problems via hyperbolic relaxation, Calcolo 25 (3) (1988) 219–232 (1989).
[31] R. H. Nochetto, A. Schmidt, C. Verdi, Adapting meshes and time-steps for phase change problems, Atti Accad. Naz. Lincei Cl. Sci. Fis. Mat. Natur. Rend. Lincei (9) Mat. Appl. 8 (4) (1997) 273–292.
[32] R. H. Nochetto, A. Schmidt, C. Verdi, A posteriori error estimation and adaptivity for degenerate parabolic problems, Math. Comp. 69 (229) (2000) 1–24.
[33] K. Nazridoust, G. Ahmadi, Computational modeling of methane hydrate dissociation in a sandstone core, Chemical Engineering Science 62 (22) (2007) 6155 – 6177.
[34] I. N. Tsimpanogiannis, P. C. Lichtner, Parametric study of methane hydrate dissociation in oceanic sediments driven by thermal stimulation, Journal of Petroleum Science and Engineering 56 (1-3) (2007) 165 – 175, natural Gas Hydrate / Clathrate.